A abyssal carbonate compensation depth overshoot in the aftermath of the Paleocene-Eocene Thermal Maximum

Donald E. Penman
Sandra Kirtland Turner
Philip F. Sexton
Richard D. Norris
Alexander J. Dickson
Slah Boulila
Andy Ridgwell
Richard E. Zeebe
James C. Zachos
Adele Cameron
Thomas Westerhold
Ursula Röhl

During the Paleocene-Eocene Thermal Maximum (PETM) about 56 million years ago, thousands of petagrams of carbon were released into the atmosphere and ocean in just a few thousand years, followed by a gradual sequestration over approximately 200,000 years. If silicate weathering is one of the key negative feedbacks that removed this carbon, a period of calcium carbonate saturation greater than pre-event levels is expected during the event's recovery phase. In the geologic record, this could be recorded as a temporary deepening of the ocean depth below which no calcite is preserved - the calcite compensation depth (CCD). Previous and new sedimentary records from sites that were above the pre-PETM calcite compensation depth show enhanced carbonate accumulation following the PETM. A new record from an abyssal site in the North Atlantic that lies below the pre-PETM calcite compensation depth shows a period of carbonate preservation beginning about 70,000 years after the onset of the PETM, providing the first direct evidence for an over-deepening of the calcite compensation depth. This record confirms an overshoot in ocean carbonate saturation during the PETM recovery. Simulations with two earth system models

support scenarios for the PETM that involve both a large initial carbon release followed by prolonged low-level emissions, consistent with the timing of CCD deepening in our record. Sequestration of these emissions was most likely the result of both globally enhanced calcite burial above the calcite compensation depth and, at least in the North Atlantic, by a temporary over-deepening of the calcite compensation depth.

The Paleocene-Eocene Thermal Maximum (PETM; ~56 Ma) represents one of the largest and most abrupt greenhouse warming events in Earth history. Marine and terrestrial records document a global >2.5‰ negative carbon isotope excursion (CIE)[1-3] coincident with global mean surface ocean warming of >4°C[4] and geochemical and sedimentological evidence for ocean acidification[5,6]. Collectively, these lines of evidence suggest a rapid (10^3-10^4 years) and massive (~3,000-10,000 PgC) release of ^{13}C-depleted carbon into the ocean-atmosphere system[7-9]. The PETM thus offers the opportunity to examine the response and recovery of the global carbon cycle and seawater carbonate chemistry to an ancient CO_2 release similar in magnitude to ongoing anthropogenic fossil fuel combustion[10].

Current understanding of long-term carbon cycle processes predicts that rapid carbon injection should cause a short-term (0-10^4 years) period of ocean acidification featuring reduced seawater carbonate saturation (Ω), followed by a longer-term (10^4-10^5.years) period of carbonate oversaturation due to elevated terrestrial silicate weathering rates (see Box 1). This carbonate saturation overshoot manifests itself in several carbon cycle model simulations of the PETM[9,11] as an over-deepening of the CCD relative to its

pre-event depth. Yet no records exist from deep sites below the pre-PETM CCD with which to detect possible CCD over-deepening. Deep-sea sedimentary records from above the CCD (Southern Ocean Site 690 [12-15] at ~1900m paleodepth and South Atlantic Sites 1263[5,14,15] at ~1500m paleodepth and 1266[5,16] at ~2500m paleodepth) show increases in $CaCO_3$ content and accumulation rate during and after the PETM recovery[13-15]. These records are consistent with weathering feedbacks prompting increased carbonate burial during the PETM recovery. These supra-CCD records are important constraints because the long-term requirement to balance the elevated weathering flux only requires carbonate burial to increase globally (not necessarily buried at deeper depths), and it is theoretically possible to accommodate such elevated global carbonate burial without substantial deepening of the CCD[17]. Nonetheless, some models[9-11] predict that a testable facet of the recovery process from massive carbon cycle perturbation involves an over-deepening of the CCD, and the location of these sites above the pre-PETM CCD means that they cannot directly test for this predicted CCD over-deepening. Direct observational evidence sites deep enough to test for a post-PETM CCD overshoot has thus far remained elusive.

New records from the North Atlantic

Here we present lithology, $CaCO_3$ content, and carbon isotope ($\delta^{13}C$) records from recently recovered sediment cores in the North Atlantic (IODP Sites U1403, PETM paleodepth ~4374m and U1409, paleodepth ~2913m[18]) that provide important constraints on the evolution of the CCD through the PETM, including the first evidence for CCD over-deepening during the PETM recovery. To explore the broader implications of these records for PETM carbon emissions scenarios, we present new carbon release experiments using

two carbon cycle models – LOSCAR[9,19] and cGENIE[20,21] and discuss uncertainties in the representation of geological carbon cycling in current models.

At Site U1409, the PETM CIE occurs in an interval of variously silicified sediments (siliceous claystones, siliceous limestones and cherts) at 178.9-179.2 mcd (Figure 1A), contrasting with the nannofossil chalk that characterizes much of the Paleogene at this site[18]. Although likely somewhat condensed, the $\delta^{13}C_{carb}$ record bears the typical[15] PETM CIE pattern of an abrupt decrease (here of ~2‰) followed by a plateau of low values and then gradual recovery (Fig. 1). Bulk $\delta^{13}C_{carb}$ over the PETM CIE interval sampled a heterogeneous mixture of lithology (clay, carbonate-rich burrows within that clay, and siliceous sediments), with all three lithologies revealing significantly lower $\delta^{13}C$ within the CIE than pre-event values. The integrity of the bulk $\delta^{13}C_{carb}$ record is also supported by the close structural similarity between it and the equivalent bulk $\delta^{13}C_{carb}$ records from the Southern Ocean and Walvis Ridge (Fig. 1, 2A). The Site U1409 $\delta^{13}C$ record from benthic foraminifera is discontinuous owing to silicification across the onset and initial recovery, but minimum values within the CIE show a large (~3‰) excursion, similar to that seen in benthic records from the Southern Ocean[22] and South Atlantic[23]. Below the CIE, carbonate content is between 60-70 wt%, decreases to a minimum of ~40 wt% at the CIE onset, and rebounds to ~70% following the CIE. This pattern is similar to other pelagic PETM sections[24] and implies that the local CCD was always deeper than the paleodepth of Site U1409, while the decrease in carbonate during the PETM can be interpreted as a transient decrease in the calcite saturation state, Ω, consistent with shoaling of the CCD. The absence of near-0 wt% $CaCO_3$ sediment at Site U1409 contrasts with records from the South Atlantic Ocean[5] where cores even shallower than U1409 are barren of carbonate within the

CIE. Although this observation could imply that CCD shoaling in the North Atlantic was less dramatic than that in the South Atlantic, hiatuses, bioturbation by burrowing, or incomplete recovery of this silicified interval could have obscured or resulted in the loss of the interval containing the lowest wt% $CaCO_3$ values. Regardless, carbonate content and accumulation rate at Site U1409 were higher during the PETM recovery than before the event, similar to other sites at mid-ocean depths or shallower[5,12-14,16], thus providing support for elevated saturation states and increased carbonate burial above the CCD during the recovery phase.

Lower abyssal Site U1403 features a prominent transition (over ~5 cm) from carbonate-poor (<0.5 wt%) claystone in the Upper Paleocene (extending from the P-E boundary to at least ~61 Ma[18]) to carbonate-bearing (~20-30 wt%) nannofossil claystone in the lower Eocene (Figure 1B). This carbonate-rich interval contains calcareous nannofossils of zone NP9B, including PETM excursion taxa *Discoaster araneus* and *Rhomboaster* spp[18]. Bulk $\delta^{13}C_{org}$ reveals a negative CIE between 200.7 and 201.5 mcd that is superimposed on comparatively high amplitude orbital timescale variability in the late Paleocene. The $\delta^{13}C_{carb}$ record necessarily begins at the onset of carbonate sedimentation with low values of ~0.6‰, followed by a gradual 1.4‰ increase over the next ~1.6 m, parallel to the recovery in $\delta^{13}C_{org}$. Given the simultaneous trends to higher values in both $\delta^{13}C_{carb}$ and $\delta^{13}C_{org}$ within zone NP9B, this $\delta^{13}C$ increase can be unambiguously assigned to the PETM CIE recovery. The magnitude of the $\delta^{13}C_{carb}$ increase (1.4‰) is close to the full amplitude of the PETM CIE recovery observed in bulk carbonates globally[15] and at Site U1409 (Figure 2A), so we confidently assign the onset of carbonate sedimentation at Site U1403 to early in the PETM recovery phase.

We construct age models by correlating the $\delta^{13}C_{carb}$ records to a compilation of bulk and fine-fraction $\delta^{13}C_{carb}$ on an orbitally calibrated age model[15] (Figure 2A and 2C). This age model, based on several PETM sites, produces a shorter duration of the PETM CIE than extraterrestrial ^{3}He-based estimates,[12,16] so durations here may represent minima. On this timescale, carbonate sedimentation begins at Site U1403 ~70kyr after the PETM onset and is followed by a period of elevated (20-40) wt% $CaCO_3$ that persists for a further ~150kyr. Fluctuations between 5 and 25 wt% $CaCO_3$ continue throughout the lower Eocene. Although the CIE onset at Site U1403 as defined by the somewhat noisy $\delta^{13}C_{org}$ record introduces some uncertainty around the placement of the P-E boundary, this does not affect the relative timing of the initial appearance of carbonate at this lower abyssal site, which is unambiguously assigned to the PETM recovery interval based on $\delta^{13}C_{carb}$ and the occurrence of PETM excursion-interval calcareous nannofossils.

The pattern of carbonate sedimentation at Site U1403 (carbonate-barren in the Paleocene with carbonate appearing during the PETM recovery) has not previously been observed in sediments spanning the PETM. The absence of carbonate in the Upper Paleocene and into the earliest Eocene indicates the CCD lay shallower than Site U1403 before the PETM and through the CIE onset and body. The onset of carbonate sedimentation ~70kyr after the PETM onset indicates that the CCD over-deepened to below the ~4400 m lower abyssal paleo-water depth of Site U1403 during the early phase of PETM recovery – direct evidence for a post-PETM CCD overshoot. The ~150kyr period of elevated carbonate deposition at Site U1403 represents the main phase of the CCD over-deepening, and is coeval with enhanced carbonate accumulation and preservation at shallower paleodepths documented here at Site U1409 and elsewhere[5,13,14,16] (Figure 2D).

These observations strongly implicate elevated whole-ocean saturation state as the cause of enhanced carbonate burial at all water depths and from the North Atlantic to the Southern Ocean.

Implications of a CCD overshoot explored with carbon cycle models

To explore the implications of a CCD overshoot and its timing, and the CCD over-deepening at U1403 in particular, we tested a variety of PETM carbon emissions scenarios using the models LOSCAR and cGENIE. Rather than carry out an extensive sweep of all combinations of plausible size and duration of carbon release, our emissions scenarios are based on ref. [9], characterized by an initial C input ($\delta^{13}C$ = -50‰) of 3000 PgC over 5 kyr, followed by 1480 PgC over 50 kyr, and originally developed to best match records of carbonate dissolution (particularly in the South Atlantic[5]). However, we explored a number of variations on this basic emissions trajectory (Figs. S4-S15) such as doubling the total mass with half the isotopic composition ($\delta^{13}C$ = -25‰). In order to isolate the response of carbonate burial dynamics from circulation effects that might diverge in the two models, we ran cGENIE with radiative forcing (and thus ocean circulation) fixed, and for direct comparison with cGENIE (Figure 3) we omitted the prescribed circulation changes of ref. 9 in LOSCAR. We tracked the evolution of global sedimentary wt% $CaCO_3$ preserved, and simulated the expected marine sediment record in modeled 'cores' at North Atlantic depths approximating Sites U1409 and U1403.

The configurations of both LOSCAR and cGENIE models used here include a CO_2-dependent silicate weathering feedback (see methods). Both models simulate a global CCD and wt% $CaCO_3$ overshoot which occurs between 20 and 45 kyr after the onset of carbon emissions and peaks between 65 and 97 kyr after the onset, depending on the emissions

schedule and model (Figure 3 and Figure S3)[9,11]. The carbonate overshoot begins earlier when the carbon pulse occurs over a shorter interval of time (Figures S6, S12). The long delay (~70kyr) in the onset of carbonate sedimentation at Site U1403 that we infer from our age model is hence difficult to reconcile with only a short "spike" of carbon released at the onset of the PETM. Rather, the delay is better explained by a sustained release of carbon lasting many tens of kyr after an initial spike (Figure 3, S1), consistent with the conclusions of refs. [9] and [6]. Such sustained carbon release might arise as a feedback response to initial warming[25,26] or represent prolonged North Atlantic volcanism. Our experiments also demonstrate that the timing of the overshoot is not particularly sensitive to the mass of carbon released – doubling the mass of carbon results in < 2 kyr delay in overshoot timing (e.g. Figure S4 vs. Figure S5).

While both models generate a whole-ocean carbonate burial overshoot during the recovery interval, the spatial distribution of $CaCO_3$ content in sediments shows differences both between the models and in comparison to Sites U1403 and U1409 (Figure 3). Because LOSCAR has much coarser spatial resolution (e.g. it represents the deep Atlantic as a single box), regional patterns need to be interpreted with greater caution. Nevertheless, LOSCAR generates a deep (4500m) $\%CaCO_3$ overshoot comparable to that seen at Site U1403, but in shallow sediments (3000m) generates a larger $\%CaCO_3$ decrease (to near-zero) and smaller overshoot than seen at Site U1409. In contrast, cGENIE closely matches the Site U1409 record, but at 5000m, sediments overshoot their pre-event $\%CaCO_3$ levels by only ~1%, in conflict with the Site U1403 record. It appears that in response to enhanced weathering-driven elevated saturation states, LOSCAR accommodates greater global carbonate burial with higher $\%CaCO_3$ in deep sediments (an over-deepening of the CCD),

193 whereas cGENIE accommodates greater global carbonate burial predominantly within and
194 above the lysocline. Observational evidence (in the form of new and previous carbonate
195 accumulation rate records) suggest that in the real world (at least in the case of the PETM),
196 both of these processes may operate.

197 The differences between the models' predictions for the locus of intensified
198 carbonate burial result from of how the models represent sedimentary processes. In
199 cGENIE, the respiration of organic carbon in sediments reduces porewater saturation state
200 and dissolves $CaCO_3$ even in shallow sediments well above the carbonate saturation
201 horizon. Because of this, those shallow sediments have greater potential to accommodate
202 an increase in $CaCO_3$ content in response to higher bottom water saturation state such as
203 that seen in the aftermath of the PETM. cGENIE thus balances enhanced weathering flux
204 via elevated carbonate burial mostly in shallow sediments (within and above the
205 lysocline)[17]. Conversely, $\%CaCO_3$ in sediments above the lysocline in LOSCAR is set by
206 the ratio of clay to $CaCO_3$ in the sediment rain (81% $CaCO_3$ in the present configuration)[19],
207 so when saturation state increases those shallow sediments cannot accommodate higher
208 $CaCO_3$ contents (they are already at a maximum). Hence, LOSCAR balances an increase
209 in weathering flux via enhanced carbonate burial within the lysocline and below the (pre-
210 event) CCD.

211 A notable aspect of the Site U1403 carbonate record is that following the main
212 phase of the CCD over-deepening featuring the highest carbonate contents, wt% $CaCO_3$
213 does not return to 0% (its pre-event level) before the next major hyperthermal (ETM-2,
214 ~2Myr later[18]) (Fig. 1, 2). Hence, the North Atlantic CCD did not return to its pre-PETM
215 state. Two possible explanations exist for this observation. First, negative feedbacks on

carbonate undersaturation could have been very slow to re-establish equilibrium. This is unlikely, given that all other records of environmental and carbon-cycle perturbation during the PETM (such as temperature[4], pH[27], and the CIE[15]) recovered in hundreds of thousands of years, not millions. Second, the carbon cycle might have transitioned to a new equilibrium state featuring a deeper CCD. Several mechanisms may help explain a deeper post-PETM equilibrium CCD in the North Atlantic. Importantly, the PETM CCD evolution may have been superimposed on a long-term (multi-million year) global CCD deepening trend[28-31]. Increasing pCO_2 on multi-million year timescales across the Late Paleocene-Early Eocene from greater volcanic CO_2 release or an imbalance between terrestrial C_{org} oxidation and marine C_{org} burial could have strengthened weathering rates, thus increasing seawater carbonate saturation and driving a gradual CCD deepening from ~58 to ~52Ma, independently of the PETM[28]. Indeed, LOSCAR simulations of carbon release superimposed on gradual long-term CCD deepening (Figure S2) agree well with observations from Site U1403, including the persistence of the overshoot.

Another possibility is that changing ocean circulation or regional carbonate export across the PETM affected the regional North Atlantic CCD (i.e. the observed CCD over-deepening was not necessarily global). Weakened North Atlantic-sourced overturning during the acidification phase followed by strengthened overturning during the oversaturation phase could have produced the initial large CCD shoal documented at Walvis Ridge[5] (South Atlantic) and the later CCD over-deepening at Site U1403 (North Atlantic). If such circulation changes persisted for several Myr, they could have produced a persistently deeper post-PETM North Atlantic CCD. Spatial benthic $\delta^{13}C$ gradients can shed light on circulation changes[22], because the accumulation of respired C_{org} reduces the

239 $\delta^{13}C$ of deep water DIC as it ages. Owing to its location in the lower abyss, Site U1403 is
240 unfortunately nearly barren of benthic foraminifera throughout the PETM and its recovery.
241 However, Site U1409 benthic $\delta^{13}C$ values overlap with those of South Atlantic[23] and
242 Southern Ocean[22] during intervals immediately prior to the PETM and during the later
243 stages of the recovery, including the time interval (>110kyr after the event) during which
244 Site U1403 documents a CCD overshoot (Figure 2). Benthic gradients between the South
245 and North Atlantic therefore do not show any evidence for large-scale changes in Atlantic
246 overturning circulation during the PETM recovery that could have contributed to a
247 localized CCD over-deepening.

248 It is also possible that the CCD over-deepening was influenced by other carbon
249 sequestration processes operating during the PETM recovery that removed carbon from the
250 ocean/atmosphere and increased seawater pH and saturation state (in a sense, the opposite
251 of the PETM acidification phase), and hence influence the CCD. In particular, studies have
252 suggested that the pace of the CIE recovery, which is complete within ~150kyr[12,16], is too
253 rapid to be explained by enhanced weathering and carbonate burial alone. Instead, the
254 preferential removal of ^{12}C via enhanced burial of organic carbon (C_{org}) has been proposed
255 to explain the CIE recovery timing[32]. This is consistent with evidence of increased marine
256 productivity during the PETM from elevated biogenic barium accumulation rates[33,34] and
257 coccolith Sr/Ca[35]. Our model experiments focus on the long-term inorganic carbon cycle
258 and silicate weathering and hence cannot exclude a role for enhanced organic carbon burial.

259 In summary, our finding of a post-PETM CCD overshoot in the North Atlantic
260 Ocean constitutes the first evidence for post-PETM variations in carbonate burial from
261 sediments deeper than the pre-PETM CCD. It thus represents an important constraint on

the vertical extent of the CCD's response to carbon release during the PETM and consequently, the processes responsible for restoring the carbon cycle to steady state. It is tempting to use this constraint to directly calculate the mass of carbon released during the PETM because the excess carbonate burial should scale with the mass of carbon released. However, we recognize that one site does not fully constrain the global extent of the overshoot, nor its absolute magnitude. Further constraints on the CCD over-deepening from even deeper water depths and additional ocean basins are therefore an essential target for future scientific drilling. Additionally, uncertainty in strength of the silicate weathering feedback (Figure S2)[36] as well as the potential influences of initial carbon cycle conditions, circulation changes, C_{org} burial, and changing clay flux preclude explicit calculation of the total carbon release[10]. Indeed, the differing responses of the two different global carbon cycle models we have tested against the observations underscore the lack of consensus on how the marine carbonate carbon sink responds in detail (and particularly in the depth distribution of $CaCO_3$ burial) to perturbation. Multiple combinations of mass and rate of carbon release, weathering feedback strength, and C_{org} burial are consistent with the new observations described here. Our findings nevertheless provide an important constraint on how carbon was sequestered in the aftermath of the PETM, an event that continues to guide our understanding of Earth system processes and feedbacks during large-scale carbon cycle perturbations.

Author Contributions: DEP, SKT, PFS, RDN, and SB conceived the study and participated in IODP Expedition 342 that recovered and described the sediments used here. DEP generated carbonate stable isotope analyses in the lab of JCZ, and AJD

generated organic carbon stable isotope and Coulormat %$CaCO_3$ analyses. XRF scanning records were generated by SKT at Scripps, and AC, PFS, TW, and UR at MARUM. DEP and SKT performed the carbon cycle modeling with guidance from REZ and AR. DEP wrote the manuscript with help from SKT and PFS, and all authors edited the manuscript.

Corresponding author: Correspondence and requests for materials should be addressed to Donald E. Penman (donald.penman@yale.edu).

METHODS

Geochemical analyses

During IODP Expedition 342, drilling operations penetrated the P-E boundary at Sites U1403 (39°56.5997N, 51°48.1998W, 4946m depth) and U1409 (41°17.7501N, 49°13.9996W, 3502m depth). Shipboard investigation described lithology, identified the approximate positions of the P-E boundary by nannofossil biostratigraphy, and provided coarse-resolution records of wt% $CaCO_3$. The surface of core archive halves spanning the PETM were scanned at 1-2 cm-resolution at the MARUM – Center for Marine Environmental Sciences, University of Bremen and at Scripps Institution of Oceanography using Avaatech X-ray fluorescence (XRF) core scanners. Estimates of the total abundance of calcium (Ca) and iron (Fe) were obtained by scanning cores at an energy level of 10kV, current of 500 uA, count time of 20 sec, and measurement area of 10 x 12 mm. Estimated wt% $CaCO_3$ records were generated by regressing shipboard wt% $CaCO_3$ measurements[18] against the natural logarithm of XRF-derived Ca/Fe ratios. For stable isotope analyses, samples were collected at ~5cm resolution from Site U1409 and

10cm resolution from Site U1403, freeze dried, homogenized with mortar and pestle, and analyzed for $\delta^{13}C_{carb}$ on a ThermoFisher MAT 253 stable isotope mass spectrometer coupled to a Kiel IV carbonate device using standard dual-inlet techniques (typical long-term $\delta^{13}C_{carb}$ reproducibility of carbonate standards is < ±0.5‰, 1 S.D.) In addition, samples from Site U1409 were washed and sieved, and specimens of the benthic foraminifera *Nuttalides truempyi* were picked from the 150-200 and 212-300μm size fraction. Where possible, 3-8 of these specimens from each sample were run using the $\delta^{13}C_{carb}$ methods described above. For $\delta^{13}C_{org}$ analysis of Site U1403, homogenized sample powders were de-carbonated in 1M HCL and washed in de-ionized water. $\delta^{13}C_{org}$ was measured using a Thermo-Finnegan MAT 253 mass spectrometer coupled to a Thermo Scientific 2000 HT elemental analyzer via a Conflo IV interface optimized for the measurement of samples with low organic carbon abundances. Analytical reproducibility was monitored using analyses of IAEA CH-6 sucrose and was < ±0.1‰ (1 S.D). All $\delta^{13}C$ data are expressed relative to V-PDB. Additional Site U1403 wt. % $CaCO_3$ was measured using a Strohlein Coulormat.

Carbon cycle modeling

LOSCAR is a numerically-efficient geochemical box model of the marine carbon cycle with realistic interaction with sediments, capable of multi-million year simulations of carbon cycle processes including CCD depth. All runs use Paleogene LOSCAR setup[19]. Code availability: the C code for the LOSCAR model can be obtained from author REZ upon request (zeebe@hawaii.edu). cGENIE is an intermediate-complexity Earth system model including a 3-D dynamic ocean model with biogeochemical cycling of key elements and isotopes and a spatially resolved sediment model capable of

generating virtual sediment cores – synthetic stacks of deep-sea sediments[20,21,37]. We use the late Paleocene/early Eocene configuration of ref. [38]. For this study, we evaluate virtual sediment core results from a depth transect in the North Atlantic ranging from 5000-3000 m water depth and at locations corresponding to Expedition 342 sites.

Both models include carbonate and silicate weathering feedbacks. In LOSCAR, weathering is parameterized as $F_w = F_{eq} * ([CO_2]_{atm} / [CO_2]_{eq})^{Nsi}$, where F_{eq} and $[CO_2]_{eq}$ are equilibrium weathering flux and atmospheric pCO_2 at which volcanic carbon emissions are perfectly balanced by silicate weathering and carbonate burial[19]. N_{Si} sets the strength of the silicate weathering feedback (default $N_{Si} = 0.2$). We implement the same formulation for a CO_2-dependent carbonate and silicate weathering feedback in cGENIE using a model for terrestrial rock weathering[39]. Following ref. [40], we assume carbonate weathering proportional to the square root of $[CO_2]_{atm} / [CO_2]_{eq}$ and silicate weathering proportional to $[CO_2]_{atm} / [CO_2]_{eq}$ raised to the power of 0.3. We assume a 50:50 split between carbonate and silicate weathering in order to match total carbonate burial, and balance silicate weathering with volcanic outgassing. We utilize the cGENIE and LOSCAR models in this study in order to qualitatively demonstrate what mechanisms are consistent with the new data, not in an attempt to reconstruct exactly a PETM scenario.

Data: Accompanying data can be found at [PANGEA web address forthcoming]

FIGURE CAPTIONS

Figure 1: Lithology and $\delta^{13}C$ over the PETM at Sites U1409 (A) and U1403 (B) plotted against composite depth (mcd). Each panel shows core photo (Site U1403 vertically

compressed), lithologic description, calcareous nannofossil biostratigraphy, wt. %$CaCO_3$ estimated by XRF scanning data (black line), and bulk $\delta^{13}C_{carb}$ (blue line). Lithology codes for Site U1409: NC = nannofossil chalk, CNC = clayey nannofossil chalk, SL = siliceous limestone, Cl = claystone, SC = siliceous claystone, Ch = chert. Bulk $\delta^{13}C_{org}$ (green line) and wt. % $CaCO_3$ measured with a Coulormat device (black X's) are also shown for Site U1403, and benthic foraminifer *Nuttalides truempyi* $\delta^{13}C$ (red squares) is shown for Site U1409. The heterogeneous mixture of clay- and carbonate-rich facies within the CIE at Site U1409 is interpreted as carbonate-rich burrows within clay-rich sediments, with both recording low (<0.5‰) bulk $\delta^{13}C$. Depth intervals representing the Paleocene, CIE, Recovery, and post-PETM based on $\delta^{13}C$ stratigraphy are highlighted with grey, red, orange, and white shaded bars, respectively. PETM phases nomenclature from ref. 15.

Figure 2: Age models and PETM isotopic and sedimentological records from new and previous sites. A: Bulk $\delta^{13}C_{carb}$ records from Sites 690[13], 1263[15], U1403, and U1409 plotted on the age model used in this study. B: Weight %$CaCO_3$ of Sites U1403 and U1409 (this study), 690[13], and 1263[5]. C: Linear sedimentation rates used in age models constructed by this study for Sites U1403 and U1409, and Sites 690 and 1263 from Röhl, et al. [15] D: Carbonate mass accumulation rate calculated from dry bulk density, sedimentation rates (C), wt. % $CaCO_3$ (B). E: Comparison of benthic foraminifer $\delta^{13}C$ from South Atlantic Site 1263,[23] Southern Ocean Site 690,[22] and U1409 demonstrating small and constant North-South aging gradient during the CCD overshoot. Green bars indicate silicified intervals at Site U1409 which precluded measurement of benthic foraminifers. In (B), (D) and (E), the

376 silicified interval of U1409 is marked with a dashed line to reflect potential hiatuses or
377 incomplete recovery which may have resulted in an incomplete %$CaCO_3$ record (see text).
378
379 **Figure 3:** Comparison of LOSCAR and cGENIE C release experiments using the
380 Emissions scenario of ref. 9 with radiative forcing (and thus circulation) fixed in
381 cGENIE, and no circulation changes in LOSCAR. Top panel: Emissions scenario. Middle
382 panel: modeled 3000m sediment core-top %$CaCO_3$ compared with Site U1409 %CaCO3
383 record. Bottom panel: modeled 4500m (LOSCAR) and 5000m (cGENIE) sediment core-
384 top %$CaCO_3$ compared with Site U1403 %CaCO3 record. In middle and bottom panels,
385 thin, opaque traces mark pre-event %$CaCO_3$ for cGENIE and LOSCAR.
386
387 **Box 1: The ocean's two-phase response to rapid carbon injection**
388 Current understanding of long-term carbon cycle processes suggests that large-
389 scale carbon injection into the ocean-atmosphere should induce a two-phase response in
390 ocean carbonate saturation. Initially, rapid invasion of CO_2 into the ocean lowers pH and
391 carbonate saturation state (Ω) in tandem[6,38,41], resulting in dissolution of both newly
392 deposited and pre-existing carbonate sediments[5]. The result is a dramatic reduction in
393 $CaCO_3$ burial in marine sediments globally and, in places, evidence for a shoaling of the
394 calcite compensation depth (CCD, the depth below which no calcium carbonate, in the
395 form of calcite, is preserved).[5,24,42].
396 A second phase of carbonate saturation and burial response arises from elevated
397 atmospheric pCO_2 and increased global temperatures that are thought to drive an increase

398 in the rate of terrestrial carbonate and silicate rock chemical weathering[43,44], which can be
399 generalized:

400 $$CaCO_3 + CO_2 + H_2O \rightarrow Ca^{2+} + 2HCO_3^- \quad (1)$$

401 $$CaSiO_3 + 2CO_2 + 3H_2O \rightarrow Ca^{2+} + 2HCO_3^- + H_4SiO_4 \quad (2)$$

402 Accelerating these reactions increases the delivery of Ca^{2+} (and thus total alkalinity) and
403 dissolved inorganic carbon (DIC) to the oceans, elevating Ω. An intensification of
404 continental weathering during the PETM is supported by a pronounced increase in the
405 $^{187}Os/^{188}Os$ of seawater[45,46] and an increase in kaolinite in marine sediments[47]. However,
406 although the silicate weathering rate responds quickly to increased temperature/CO_2, the
407 rate of CO_2 drawdown from global weathering (~ 0.1 PgC/yr[41]) is small in comparison to
408 estimates of initial carbon release (thousands of PgC)[7-9], meaning that this feedback should
409 take $>10^4$ years to gradually overcome the undersaturation associated with the initial
410 acidification phase[11,48,49]. On longer timescales ($>10^5$ years)[49], this increased weathering-
411 derived flux of TA and DIC to the oceans must be balanced by carbonate production and
412 burial to balance the ocean's alkalinity budget:

413 $$Ca^{2+} + 2HCO_3^- \rightarrow CaCO_3 + CO_2 + H_2O \quad (3)$$

414 The long-term balance of carbonate weathering with carbonate burial has no permanent
415 effect on the ocean's TA or DIC budgets (Equation 1 is simply the reverse of Equation 3).
416 However, the long-term balance of silicate weathering (Equation 2) with carbonate burial
417 (Equation 3) gives rise to a net consumption of CO_2 that is buried as $CaCO_3$ sediment – the
418 long-term fate of carbon released during the PETM.

419 The assumption that net CO_2 consumption (Equation 2+3) is responsive to a
420 perturbation in climate forms the basis of a proposed long-term negative (stabilizing)

feedback on climate, hypothesized to have been important in maintaining a habitable climate throughout Earth history[43,44] and specifically during the PETM recovery[11]. One way in which global carbonate burial could respond to changing weathering flux is through fluctuations of the global sea-floor area of carbonate-free sediments (i.e the CCD). In other words, during the initial acidification phase, carbonate undersaturation leads to a reduced $CaCO_3$ sink and a short-term shoaling of the CCD, whereas on longer timescales ($>10^5$ years), faster weathering rates lead to carbonate oversaturation and increased carbonate burial, which might be reflected in an over-deepening of the CCD[10,11,50]. The interval of excess (compared to pre-PETM) $CaCO_3$ burial primarily reflects the removal of carbon released at the onset of the PETM by enhanced silicate weathering, together with the quantity of $CaCO_3$ dissolved during the initial carbonate undersaturation phase and additional terrestrial weathering of carbonate rocks under warmer temperatures (both of which will be some function of CO_2 release). The characteristics of any post-PETM CCD overshoot hence potentially hold key information regarding the magnitude of carbon release and the processes involved in the recovery from an abrupt carbon cycle perturbation.

References

1 Koch, P. L., Zachos, J. C. & Gingerich, P. D. Correlation Between Isotope Records in Marine and Continental Carbon Reservoirs Near the Palaeocene Eocene Boundary. *Nature* **358**, 319-322 (1992).

2 Kennett, J. P. & Stott, L. D. Abrupt Deep-Sea Warming, Palaeoceanographic Changes and Benthic Extinctions At the End of the Palaeocene. *Nature* **353**, 225-229 (1991).

3 McInerney, F. A. & Wing, S. The Paleocene-Eocene Thermal Maximum: A Perturbation of Carbon Cycle, Climate, and Biosphere with Implications for the future. *Annual Review of Earth & Planetary Sciences* **39**, 489-516 (2011).

4 Dunkley-Jones, T. *et al.* Climate model and proxy data constraints on ocean warming across the Paleocene-Eocene Thermal Maximum. *Earth-Science Reviews* **125**, 123-145 (2013).
5 Zachos, J. C. *et al.* Rapid acidification of the ocean during the Paleocene-Eocene thermal maximum. *Science* **308**, 1611-1615 (2005).
6 Penman, D. E., Hönisch, B., Zeebe, R. E., Thomas, E. & Zachos, J. C. Rapid and sustained surface ocean acidification during the Paleocene‐Eocene Thermal Maximum. *Paleoceanography* (2014).
7 Dickens, G. R., Oneil, J. R., Rea, D. K. & Owen, R. M. Dissociation of Oceanic Methane Hydrate As a Cause of the Carbon Isotope Excursion At the End of the Paleocene. *Paleoceanography* **10**, 965-971 (1995).
8 Panchuk, K., Ridgwell, A. & Kump, L. R. Sedimentary response to Paleocene-Eocene Thermal Maximum carbon release: A model-data comparison. *Geology* **36**, 315-318 (2008).
9 Zeebe, R. E., Zachos, J. C. & Dickens, G. R. Carbon dioxide forcing alone insufficient to explain Palaeocene-Eocene Thermal Maximum warming. *Nature Geoscience* **2**, 576-580 (2009).
10 Zeebe, R. & Zachos, J. Long-term legacy of massive carbon input to the Earth system: Anthropocene vs. Eocene. *Philosophical Transactions of the Royal Society*, 1-22 (2012).
11 Dickens, G. R., Castillo, M. M. & Walker, J. C. G. A blast of gas in the latest Paleocene: Simulating first-order effects of massive dissociation of oceanic methane hydrate. *Geology* **25**, 259-262 (1997).
12 Farley, K. A. & Eltgroth, S. F. An alternative age model for the Paleocene-Eocene thermal maximum using extraterrestrial He-3. *Earth and Planetary Science Letters* **208**, 135-148 (2003).
13 Kelly, D. C., Zachos, J. C., Bralower, T. J. & Schellenberg, S. A. Enhanced terrestrial weathering/runoff and surface ocean carbonate production during the recovery stages of the Paleocene-Eocene thermal maximum. *Paleoceanography* **20**, - (2005).
14 Kelly, D. C., Nielsen, T. M. J., McCarren, H. K., Zachos, J. C. & Rohl, U. Spatiotemporal patterns of carbonate sedimentation in the South Atlantic: Implications for carbon cycling during the Paleocene-Eocene thermal maximum. *Palaeogeography Palaeoclimatology Palaeoecology* **293**, 30-40 (2010).
15 Röhl, U., Westerhold, T., Bralower, T. J. & Zachos, J. C. On the duration of the Paleocene-Eocene thermal maximum (PETM). *Geochemistry Geophysics Geosystems* **8**, - (2007).
16 Murphy, B. H., Farley, K. A. & Zachos, J. C. An extraterrestrial He-3-based timescale for the Paleocene-Eocene thermal maximum (PETM) from Walvis Ridge, IODP Site 1266. *Geochimica Et Cosmochimica Acta* **74**, 5098-5108 (2010).
17 Greene, S. *et al.* in *2014 AGU Fall Meeting Abstracts.* PP41C-1407.
18 Norris, R. *et al.* Paleogene Newfoundland sediment drifts. *Integrated Ocean Drilling Program: Preliminary Reports*, 1-263 (2012).
19 Zeebe, R. LOSCAR: Long-term ocean-atmosphere-sediment carbon cycle reservoir model v2. 0.4. *Geoscientific Model Development* **5**, 149-166 (2012).

20 Ridgwell, A. & Hargreaves, J. Regulation of atmospheric CO2 by deep‐sea sediments in an Earth system model. *Global Biogeochemical Cycles* **21** (2007).
21 Ridgwell, A. Interpreting transient carbonate compensation depth changes by marine sediment core modeling. *Paleoceanography* **22** (2007).
22 Nunes, F. & Norris, R. D. Abrupt reversal in ocean overturning during the Palaeocene/Eocene warm period. *Nature* **439**, 60-63 (2006).
23 McCarren, H., Thomas, E., Röhl, U. & Zachos, J. C. The Paleocene-Eocene Carbon Isotope Excursion: Insights from the benthic record (ODP Leg 208, Walvis Ridge). *Geophysics, Geosystems, Geochemistry* (2008).
24 Zeebe, R. E. & Zachos, J. C. Reversed deep-sea carbonate ion basin gradient during Paleocene-Eocene thermal maximum. *Paleoceanography* **22**, - (2007).
25 Zeebe, R. E. What caused the long duration of the Paleocene‐Eocene Thermal Maximum? *Paleoceanography* **26**, 1-13 (2013).
26 Bowen, G. J. Up in smoke: A role for organic carbon feedbacks in Paleogene hyperthermals. *Global and Planetary Change* **109**, 18-29 (2013).
27 Penman, D. E., Hönisch, B., Zeebe, R. E., Thomas, E. & Zachos, J. C. Rapid and sustained surface ocean acidification during the Paleocene‐Eocene Thermal Maximum. *Paleoceanography* **29**, 357-369 (2014).
28 Komar, N., Zeebe, R. & Dickens, G. Understanding long‐term carbon cycle trends: The late Paleocene through the early Eocene. *Paleoceanography* **28**, 650-662 (2013).
29 Leon-Rodriguez, L. & Dickens, G. R. Constraints on ocean acidification associated with rapid and massive carbon injections: The early Paleogene record at ocean drilling program site 1215, equatorial Pacific Ocean. *Palaeogeography, Palaeoclimatology, Palaeoecology* **298**, 409-420 (2010).
30 Hancock, H. J., Dickens, G. R., Thomas, E. & Blake, K. L. Reappraisal of early Paleogene CCD curves: foraminiferal assemblages and stable carbon isotopes across the carbonate facies of Perth Abyssal Plain. *International Journal of Earth Sciences* **96**, 925-946 (2007).
31 Slotnick, B. *et al.* Early Paleogene variations in the calcite compensation depth: new constraints using old boreholes across Ninetyeast Ridge in the Indian Ocean. *Climate of the Past Discussions* **10**, 3163-3221 (2014).
32 Bowen, G. J. & Zachos, J. C. Rapid carbon sequestration at the termination of the Palaeocene-Eocene Thermal Maximum. *Nature Geoscience* **3**, 866-869 (2010).
33 Bains, S., Norris, R. D., Corfield, R. M. & Faul, K. L. Termination of global warmth at the Palaeocene/Eocene boundary through productivity feedback. *Nature* **407**, 171-174 (2000).
34 Ma, Z. *et al.* Carbon sequestration during the Palaeocene-Eocene Thermal Maximum by an efficient biological pump. *Nature Geoscience* (2014).
35 Stoll, H. M. & Bains, S. Coccolith Sr/Ca records of productivity during the Paleocene-Eocene thermal maximum from the Weddell Sea. *Paleoceanography* **18** (2003).
36 Uchikawa, J. & Zeebe, R. E. Influence of terrestrial weathering on ocean acidification and the next glacial inception. *Geophysical Research Letters* **35** (2008).

37 Ridgwell, A. Application of sediment core modelling to interpreting the glacial-interglacial record of Southern Ocean silica cycling. *Clim Past* **3**, 387-396 (2007).
38 Ridgwell, A. & Schmidt, D. N. Past Constraints on the vulnerability of marine calcifiers to massive carbon dioxide release. *Nature Geoscience* **3**, 196-200 (2010).
39 Colbourn, G., Ridgwell, A. & Lenton, T. The Rock Geochemical Model (RokGeM) v0. 9. *Geoscientific Model Development* **6**, 1543-1573 (2013).
40 Walker, J. C. G. & Kasting, J. F. Effects of fuel and forest conservation on future levels of atmospheric carbon dioxide. *Palaeogeogr., Palaeoclimatol., Palaeoecol.* **97**, 151-189 (1992).
41 Hönisch, B. *et al.* The Geological Record of Ocean Acidification. *Science* **335**, 1058-1063 (2012).
42 Sluijs, A., Zachos, J. C. & Zeebe, R. E. Constraints on hyperthermals. *Nature Geosci* **5**, 231-231 (2012).
43 Walker, J. C. G., Hays, P. B. & Kasting, J. F. A Negative Feedback Mechanism for the Long-Term Stabilization of Earths Surface-Temperature. *J Geophys Res-Oc Atm* **86**, 9776-9782 (1981).
44 Berner, R. A., Lasaga, A. C. & Garrels, R. M. The carbonate-silicate geochemical cycle and its effects on atmospheric carbon dioxide over the past 100 million years. *American Journal of Science* **283**, 641-683 (1983).
45 Dickson, A. J. *et al.* Evidence for weathering and volcanism during the PETM from Arctic Ocean and Peri-Tethys osmium isotope records. *Palaeogeography Palaeoclimatology Palaeoecology* (in press).
46 Ravizza, G., Norris, R. N., Blusztajn, J. & Aubry, M. P. An osmium isotope excursion associated with the late Paleocene thermal maximum: Evidence of intensified chemical weathering. *Paleoceanography* **16**, 155-163 (2001).
47 Robert, C. & Kennett, J. P. Antarctic Subtropical Humid Episode At the Paleocene-Eocene Boundary - Clay-Mineral Evidence. *Geology* **22**, 211-214 (1994).
48 Goodwin, P. & Ridgwell, A. Ocean ‐ atmosphere partitioning of anthropogenic carbon dioxide on multimillennial timescales. *Global Biogeochemical Cycles* **24** (2010).
49 Lord, N., Ridgwell, A., Thorne, M. & Lunt, D. An impulse response function for the “long tail” of excess atmospheric CO2 in an Earth system model. *Global Biogeochemical Cycles* (2015).
50 Palike, H., Lyle, M., Nishi, H. & al., e. A Cenozoic record of the equatorial Pacific carbonate compensation depth. *Nature* **488**, 609-614 (2012).

Acknowledgements: We thank the scientists and crew of IODP Expedition 342 and the IODP Bremen Core Repository (BCR). We thank M. Gilmour and S. Nicoara for assistance in the stable isotope laboratory at The Open University, V. Lukies for assistance in the XRF Core Scanning laboratory at MARUM, University of Bremen ,and

D. Andreasen for assistance with carbonate stable isotope analyses at UC Santa Cruz. The comments of two anonymous reviewers greatly improved the manuscript. This work was supported by NSF OCE-1220615 to JZ and RZ and the *Deutsche Forschungsgemeinschaft* (DFG) to UR and TW.

623 Fig.1

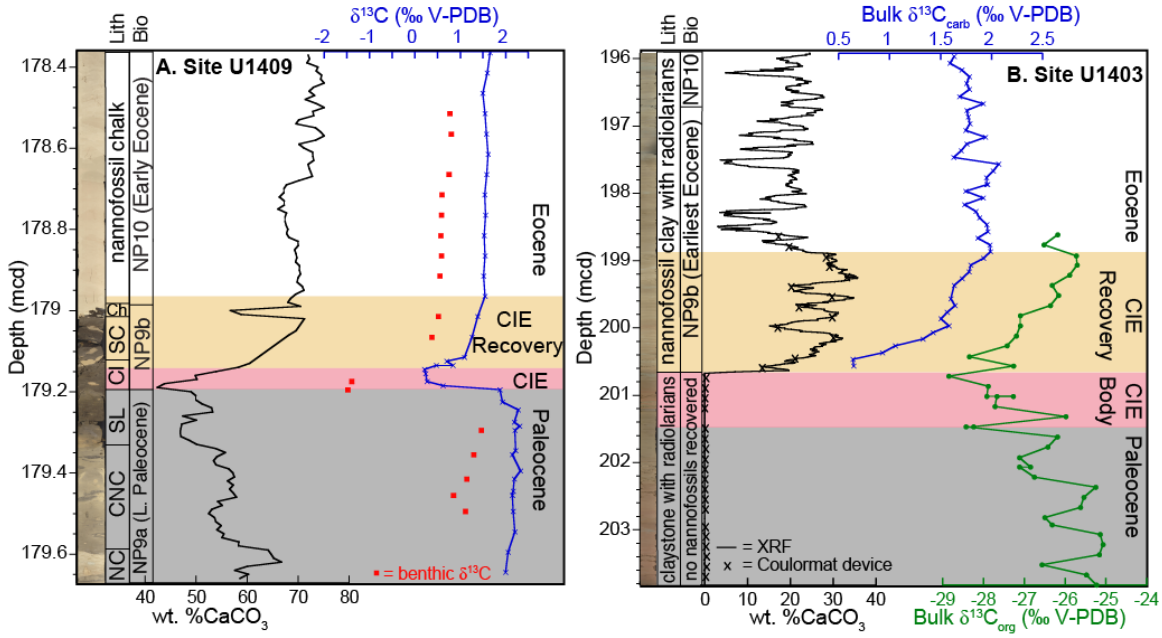

624
625
626
627
628
629
630
631
632
633
634
635
636
637
638
639
640
641
642
643
644
645
646
647
648
649
650
651
652

653 Fig. 2
654

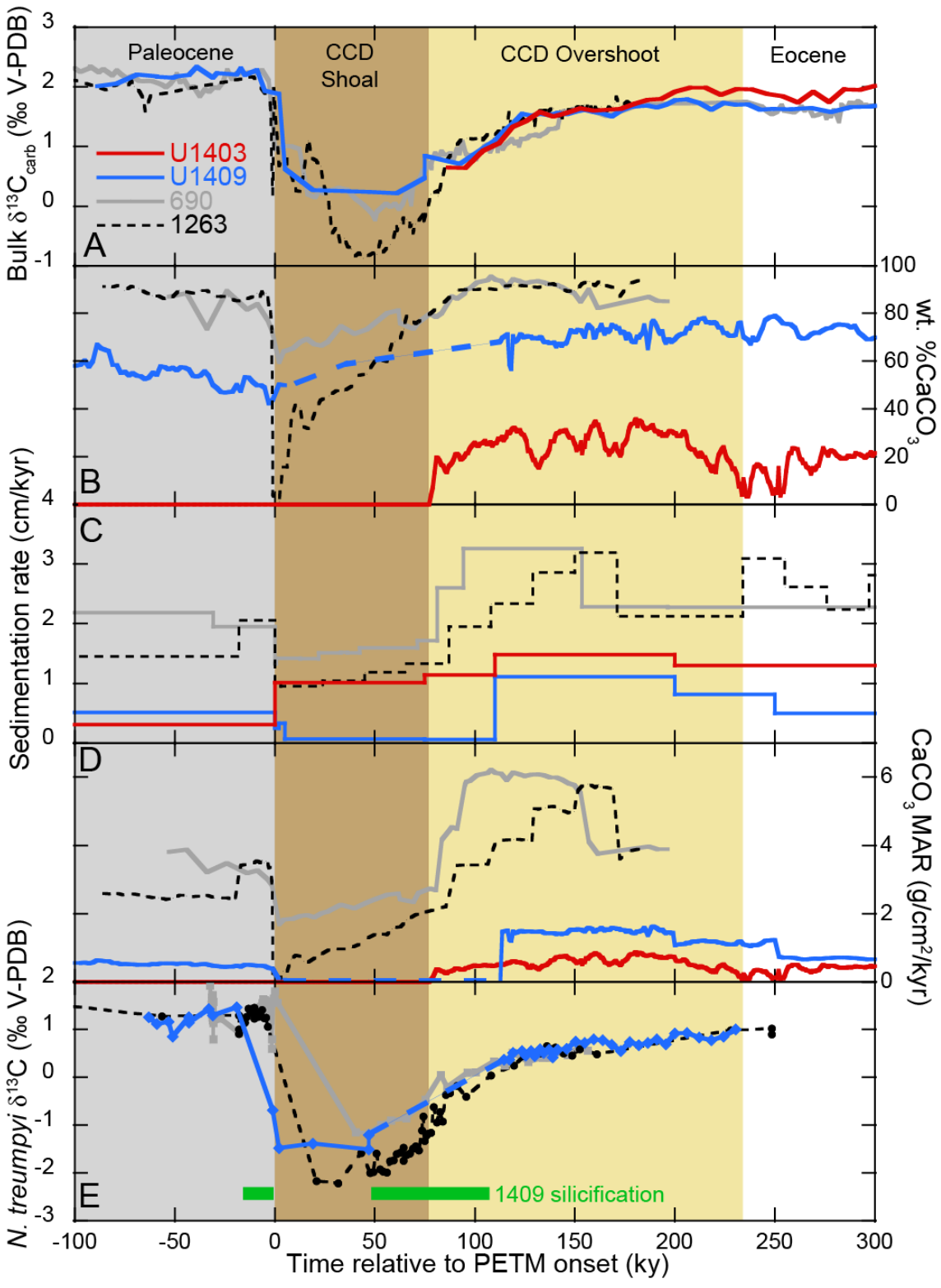

655
656
657

Fig. 3

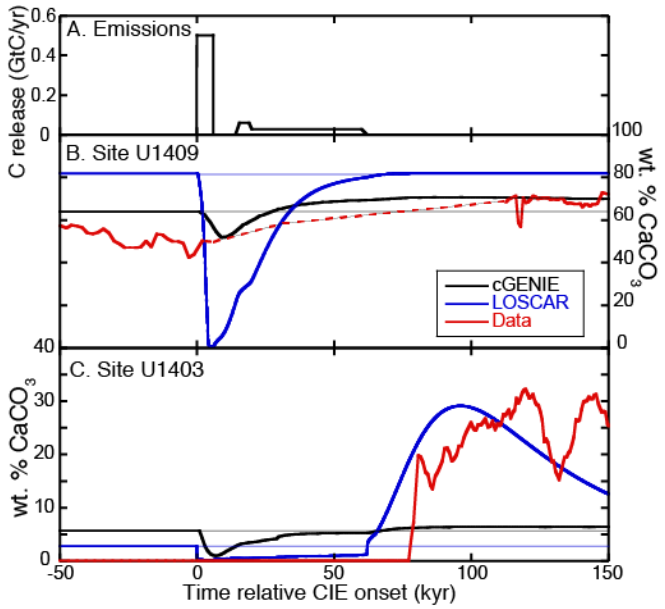
A. Emissions
B. Site U1409
C. Site U1403
C release (GtC/yr)
wt. % CaCO3
cGENIE
LOSCAR
Data
Time relative CIE onset (kyr)